Energy Levels and Crystal-Field Calculations of Europium and Terbium in Yttrium Aluminum Garnet*

J. A. KONINGSTEIN
Bell Telephone Laboratories, Murray Hill, New Jersey
(Received 1 June 1964)

Experimental and theoretical studies of the trivalent europium and terbium ions in yttrium aluminum garnet are reported in this communication. From crystal-field calculations on the split ^7F manifolds of Eu^{3+} and Tb^{3+}, it is concluded that the crystal field is approximately tetragonal. Agreement between experimental and calculated splitting patterns is satisfactory for those Stark components of ^7F manifolds which are not far removed from the center of gravity.

I. INTRODUCTION

ENERGY levels of some rare-earth ions in yttrium aluminum garnet (YAlG) and yttrium gallium garnet (YGaG) are reported in the literature.[1–6] The splitting of J manifolds of Er^{3+}:YGaG has been explained by Pappalardo[4] on the basis of a crystal field of cubic symmetry. The crystallographic data of Geller and Gilleo[7] on the position of ions in YIG indicate that yttrium ions (which are replaced by rare-earth ions) occupy sites of orthorhombic symmetry. Dillon and Walker[8] have calculated the crystal field for this site. Recent calculations on the split manifolds of Nd^{3+}:YAlG indicate[6] that the symmetry of the crystal field is approximately tetragonal. In this communication the energy level diagrams of Eu^{3+} and Tb^{3+}:YAlG are discussed. The crystal-field calculations indicate that a slight deviation occurs from tetragonal symmetry. This deviation has been found to be larger in the gallium garnet than in the aluminum garnet.

II. EXPERIMENTAL

Absorption spectra of samples containing ~5–10% Eu^{3+} and Tb^{3+}:YAlG have been studied in the infrared with a Beckman IR7 spectrometer. In the visible, a $\frac{1}{2}$-m Jarrell-Ash spectrometer was used. The fluorescence spectrum of Eu^{3+}:YAlG and Tb^{3+}:YAlG was also studied, and the fluorescence was excited with a filtered high-pressure Hg light source. The absorption and fluorescence spectra of these materials were studied at 30, 77, and 300°K.

1. Absorption Spectrum of Eu^{3+}: YAlG

The energy level diagram of the trivalent europium ion is now well known[9] for J states up to 28 000 cm^{-1}. The $^7F_1$ state has been established at ~350 cm^{-1} above the ground state $^7F_0$. The transitions in the absorption spectrum at room temperature for Eu^{3+}:YAlG originates in levels of the $^7F_0$ and $^7F_1$ manifolds.

a. Absorption Spectrum in the Visible

The transition between the $^7F_0$ and $^5D_0$ states of Eu^{3+}:YAlG should occur at about ~5810 Å. No absorption has been found in that region; however, a triplet was recorded at 5905.5, 5912.5, and 5968.5 Å (see Fig. 1). Upon cooling of the sample, this triplet disappeared, indicating that the transitions originate in excited levels. Fluorescence of Eu^{3+}:CdF_2 has been observed by Kingsley and Prener[10] in the same part of the spectrum, and they attributed it to transitions between the $^5D_0$ and $^7F_1$ manifolds, The transitions of $^7F_1$ to $^5D_0$ for Eu^{3+}:YAlG occur apparently at the three wavelengths mentioned above.

Two rather strong absorptions have been detected at 5276.5 and 5265.0 Å. The linewidth of these absorptions decreased on cooling to liquid N_2 temperature. These two bands represent transitions between the ground state and two of the Stark levels of the $^5D_1$ manifold. Other absorptions at 5345, 5350.8, and 5406.4 Å disappeared when the sample was cooled to 77°K. Transitions between levels of the $^7F_1$ and $^5D_1$ manifolds of Eu^{3+}:YAlG occur in this region. Also transitions from a level 824 ± 2 cm^{-1} above the ground state to the levels of $^5D_0$ and $^5D_1$ manifolds have been observed (300°K) at 6099.0, 5513, and 5503 Å. The absorption spectrum described up to this point enables one to set up a part of the term scheme of Eu^{3+}:$Y_3Al_2(AlO_4)_3$ (see Fig. 2). The position of the level of the $^5D_0$ state was calculated to be at $17\,220\pm5$ cm^{-1} above the ground state.

Transitions from the ground state and levels of the excited state $^7F_1$ to the crystal-field components of the $^5D_2$ and $^5D_3$ manifolds have been observed as weak absorptions between 4665 and 4045 Å. The absorption bands in the visible are given in Table I.

b. Absorption Spectrum in the Infrared

Strong absorptions have been observed in the region from 1900 to 5400 cm^{-1} at room temperature and at

* This work was supported in part by the U. S. Army Signal Corps under Contract DA-36-039-AMC-02333(E).
[1] R. Pappalardo and D. L. Wood, J. Chem. Phys. **33**, 1734 (1960).
[2] D. L. Wood, J. Chem. Phys. **39**, 1671 (1963).
[3] L. G. Van Uitert, R. C. Linares, and A. A. Ballman, J. Chem. Phys. **36**, 702 (1962).
[4] R. Pappalardo, Z. Physik **173**, 374–391 (1963).
[5] R. Pappalardo, Nuovo Cimento **26**, 4, 748 (1962).
[6] J. A. Koningstein and J. E. Geusic, preceding paper, Phys. Rev. **135**, A711 (1964).
[7] S. Geller and M. A. Gilleo, Phys. Chem. Solids **3**, 30 (1957).
[8] J. F. Dillon and L. R. Walker, Phys. Rev. **124**, 1401 (1961).
[9] G. H. Dieke and H. M. Crosswhite, Appl. Optics **2**, 7, 675 (1963).
[10] J. D. Kingsley and J. S. Prener, Phys. Rev. **126**, 458 (1962).

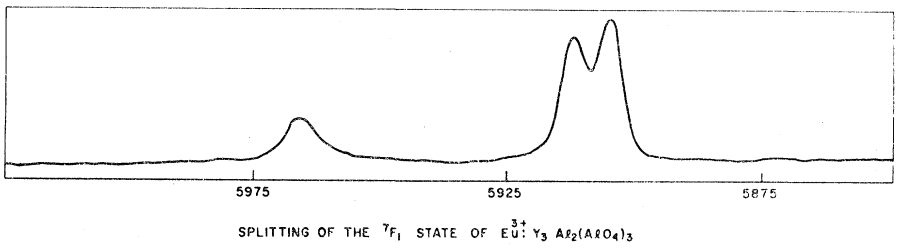

FIG. 1. The absorption spectrum of Eu^{3+}:YAlG between 5975 and 5875 Å at 300°K.

~30°K. Strong host-lattice absorptions below 1900 cm^{-1} prevent the observation of transitions between the ground state and levels of the $^7F_2$ and $^7F_1$ manifolds. Four groups of absorptions have been found in the abovementioned spectral region. Transitions from the ground state to crystal-field components of the $^7F_3$, $^7F_4$, $^7F_5$, and $^7F_6$ manifolds occur between 1916–1994 cm^{-1}; 2863–3246 cm^{-1}; 3791–4226 cm^{-1}, and 4976–5145 cm^{-1}. The part of the spectrum from 3.6–3.2 μ[2780–3230 cm^{-1}] and 2.1–1.8 μ[4760–5560 cm^{-1}] is shown in Figs. 3 and 4. The absorption spectrum of Eu^{3+}:$YGa_2(GaO_4)_3$ in the same spectral regions is also shown. A similarity between the two spectra exists, although the absorptions occur at somewhat different wavelengths. The spectra of Eu^{3+}:YAlG and Eu^{3+}:YGaG are quite similar and reveal the presence of doublets, the doublet separation in the gallium garnet being slightly larger than in the aluminum garnet. The infrared absorption bands of Eu^{3+}:YAlG are listed in Table II.

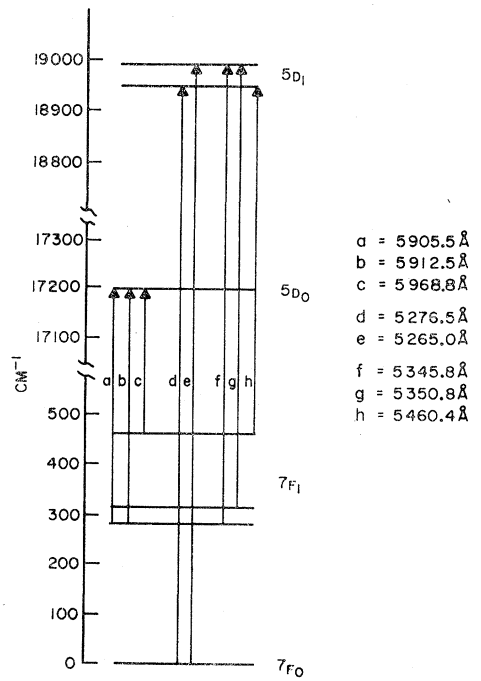

FIG. 2. Transitions of Eu^{3+}:YAlG in the spectral region of 5975–5265 Å.

2. Fluorescence Spectrum of Eu^{3+}: YAlG

The fluorescence spectrum has been recorded at room temperature and 77°K in the spectral region of 5900 to 7110 Å. Strong fluorescence occurs at 5904.9, 5912.9, and 5964 Å, which originates in the level of the $^5D_0$ state and terminates on crystal field levels of the $^7F_1$ manifold. Other fluorescence lines have been recorded at 6097 and 6304 Å and at 6533.5, 6553.0, and 6567.0 Å. These fluorescence lines originate in the $^5D_0$ state and terminate on levels of the $^7F_2$ and $^7F_3$ manifolds. Additional high-resolution, low-temperature fluorescence measurements have been made available to us by Dr. D. L. Wood of this laboratory. A sharp but weak line at 17 211 cm^{-1} is assigned to the $^5D_0$–$^7F_0$ transition. The position of $^5D_0$ state as obtained from the fluorescence measurement is to be compared with the absorption measurements in the visible at 17 220±5 cm^{-1} which was inferred from absorption measurements at room temperature (see Fig. 2). This apparent shift may be due to the fact that the fluorescence measurements were made at 77°K, while the absorption measurements were made at 300°K.

TABLE I. Absorption spectrum of Eu^{3+}:YAlG from 6100–4050 Å.

300°K (Å)	Absorptions Intensity[a]	72°K (Å)	Assignment
6099.0	w	...	$^7F_2$–$^5D_0$
5968.8	m	...	
5912.5	st	...	$^7F_1$–$^5D_0$
5905.5	st	...	
5513	w	...	
5503	w	...	$^7F_2$–$^5D_1$
5406.4	m	...	
5350.8	m	...	$^7F_1$–$^5D_0$
5345.8	m	...	
5276.5	st	5276.4 (18 952 cm^{-1})	$^7F_0$–$^5D_1$
5265.0	st	5266.0 (18 991 cm^{-1})	
4746.8	w	...	
4727.3	w	...	$^7F_1$–$^5D_2$
4722.5	w	...	
4681.0	m	4681.5 (21 356 cm^{-1})	$^7F_0$–$^5D_2$
4661.0	m	4661.5 (21 448 cm^{-1})	
4655.8	m	4656.4 (21 473 cm^{-1})	
4120	vw	...	
4108	vw	...	$^7F_1$–$^5D_3$
4102	vw	...	
4097	vw	...	
4056	w	4058.5 (24 639 cm^{-1})	$^7F_0$–$^5D_3$
		4052.5 (24 678 cm^{-1})	
		4051.5 (24 683 cm^{-1})	
4049.0	w	4049.0 (24 697 cm^{-1})	

[a] w = weak; m = medium; st = strong; vw = very weak.

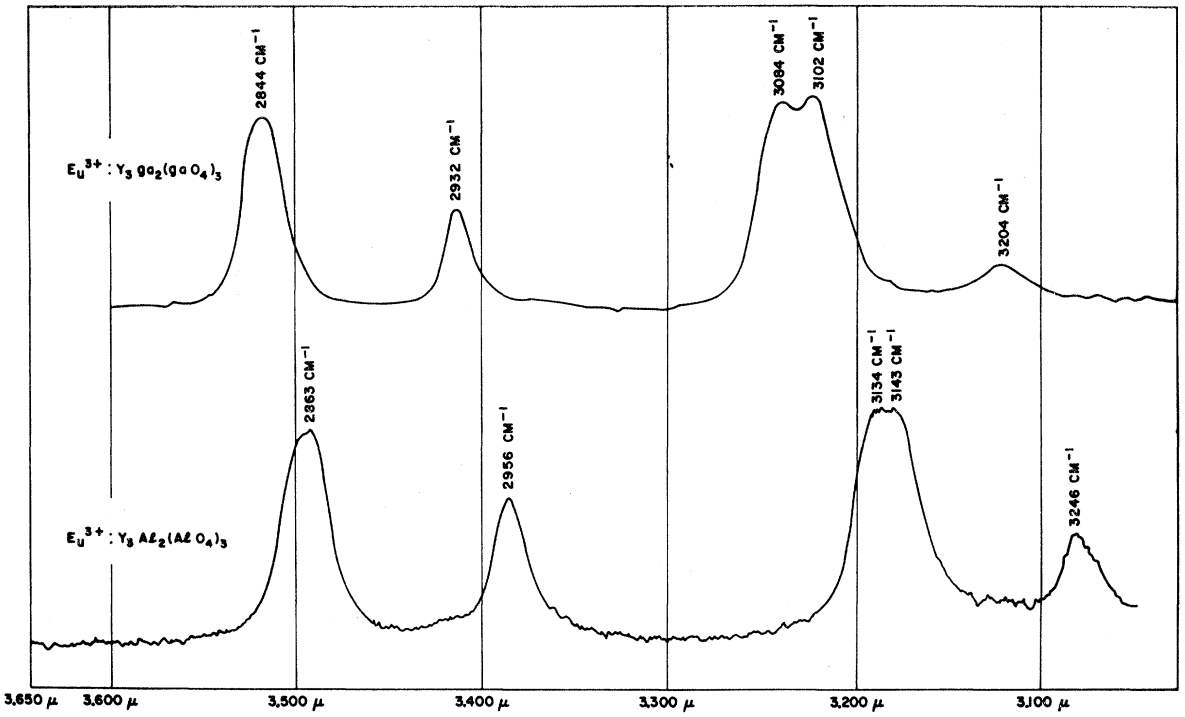

FIG. 3. The absorption spectrum of Eu^{3+}:YAlG and Eu^{3+}:YGaG between 3.6 and 3.1 μ at 30°K.

The fluorescence lines of Eu^{3+}:YAlG are listed in Table III.

3. Absorption Spectrum of Tb^{3+}: YAlG

The Tb^{3+} ion energy-level diagram is well known[9] up to 28 000 cm^{-1}. The first excited state $^7F_5$ occurs at $\sim$2000 cm^{-1}. The absorptions of Tb^{3+}:$Y_3Al_2(AlO_4)_3$ at 300°K or at lower temperatures originate from Stark levels of the $^7F_6$ manifold only.

TABLE II. The absorption spectrum of Eu^{3+}:YAlG in the infrared. Transitions originate in the $^7F_0$ level.

Absorptions (cm^{-1})	Intensity[a]	Assignment
1916	m	
1957	st	$^7F_3$
1998	m	
2863	st	
2956	m	
3134	st	$^7F_4$
3143	st	
3246	m	
3785	w	
3791	st	
3946	m	$^7F_5$
4097	m	
4226	m	
4976	st	
4983	st	
5041	st	
5151	m	$^7F_6$
5319	w	
5358	vw	
5445	vw	

[a] The intensities are relative and valid inside A group only. w = weak; m = medium; st = strong; vw = very weak.

TABLE III. Fluorescence of Eu^{3+}:YAlG. All transitions originate in the level of $^5D_0$.

Obs (Å) 300°K	Obs (Å) 77°K	Average cm^{-1}	17 220-$\tilde{\nu}$	Infrared or visible absorption	Assignment
5904.9	5905.1	16 934	286	286	
5912.4	5912.8	16 913	307	307	$^7F_1$
5964.8	5964.5	16 766	454	455	
6097.0	6096.8	16 401	819	824	
	6128[a]	16 318	902	···	
	6174[a]	16 198	1022[b]	···	$^7F_2$
6304.5	6304.0	15 862	1358	···	
	6498[a]	15 389	1832	···	
	6503[a]	13 378	1842	···	
6533.0	6534.0	16 305	1915	1916	
6553.0	6553.0	15 259	1961	1957	$^7F_3$
~6570	6571.0[a]	15 218	2002	1998	
	6574.0[a]	15 212	2008		
	6586.0[a]	14 999	2221		
	6961.8[a]	14 364	2856	2863	
	6966.2[a]	14 355	2865		
	7011.1[a]	14 263	2957	2956	$^7F_4$
7106.0	7101.7[a]	14 081	3139	3134	
	7107.3[a]	14 070	3150	3143	
	7158.1[a]	13 970	3250	3246	
	7444.3[a]	13 433	3787	3785	$^7F_5$
				3791	
	8202.0[a]	12 912	5028	5041	$^7F_6$
	8225.0[a]	12 158	5062		

[a] Photographic method.
[b] Doublet.

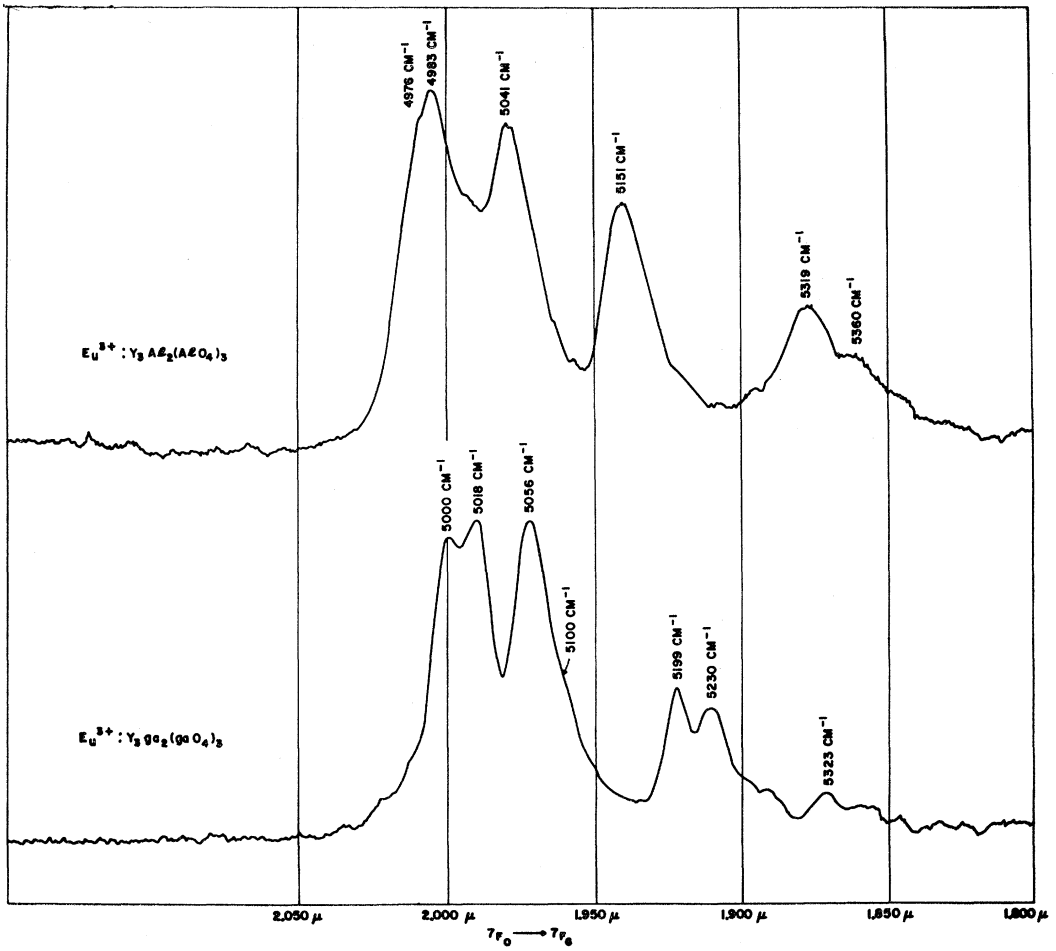

FIG. 4. The absorption spectrum of Eu^{3+}:YAlG and Eu^{3+}:YGaG between 2.05 and 1.80 μ at 30°K.

a. Absorption Spectrum in the Visible

At 300°K a complicated spectrum has been recorded in the region between 4830 and 4950 Å. At liquid helium temperature this spectrum consists of three bands, all showing fine structure. Peaks occur at 4840.0, 4843.5, 4854.0, 4857.0, and 4867.0 Å. They represent transitions from the ground state to crystal field levels within the $^5D_4$ manifold. These absorption bands are given in Table IV.

b. Absorption Spectrum in the Infrared

Groups of absorptions have been observed in Tb^{3+}:YAlG between 2000 and 5900 cm^{-1}.

The absorption spectrum between 2130–2614 cm^{-1}; 3365–3725 cm^{-1}, and 4397–4710 cm^{-1} consist of transitions which originate in the ground level and terminate on Stark levels of the $^7F_5$, $^7F_4$, and $^7F_3$ manifolds of Tb^{3+}:YAlG. Absorptions at 5010, 5611, and 5633 cm^{-1} are due to transitions which originate in the ground level and terminate on levels of the $^7F_2$ and $^7F_1$ manifolds. The level of the $^7F_0$ state of Tb^{3+}:YAlG has been established at 5882 cm^{-1} above the ground level. The absorption spectrum of Tb^{3+}:YAlG in the spectral regions of 2.5–2.1 μ and 2.05–1.65 μ is shown in Figs. 5 and 6. The spectrum of the terbium ion in the host-lattice yttrium gallium garnet in the same spectral regions is

TABLE IV. Absorptions of Tb^{3+}:YAlG in the visible.

300°K (Å)	4.2°K (Å)
4838	4840 (20 661 cm^{-1})
	4843.5 (20 646 cm^{-1})
4855.3	4854.0 (20 601 cm^{-1})
	4857.0 (20 587 cm^{-1})
4867.3	4867.0 (20 546 cm^{-1})
4871.2	...
4873.8	...
4881.7	...
4887.8	...
4908.7	...
4920.0	...
4926.0	...
4932.0	...
4942.5	...
4947.5	...

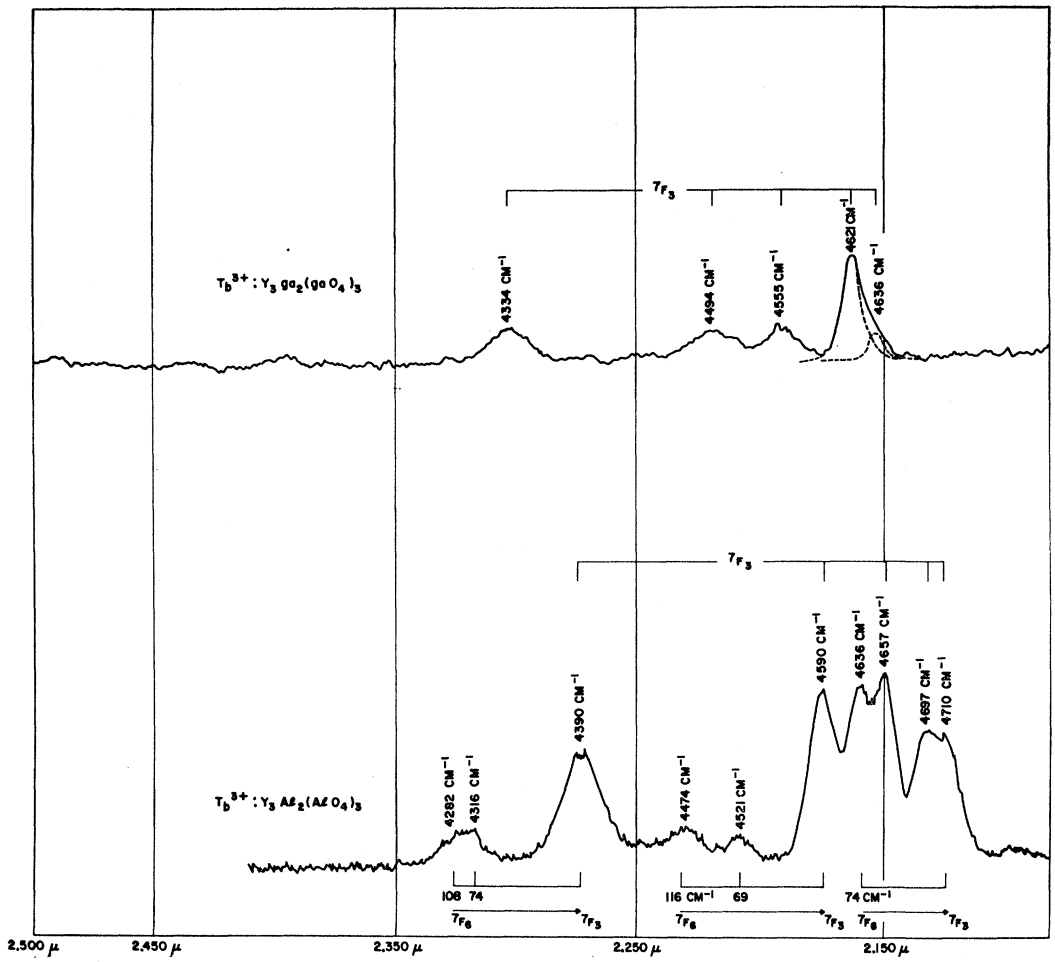

FIG. 5. The absorption spectrum of Tb^{3+}:YAlG and Tb^{3+}:YGaG between 2.1 and 2.5 μ at 30°K. Transitions in excited levels of the $^7F_6$ manifold are also indicated.

also shown. These absorption spectra were measured at 30°K. At this temperature some of the excited levels are still populated. Temperature dependence of the bands in the spectral regions as shown in Figs. 5 and 6 allows us to identify absorptions which originate in some of the Stark levels of the $^7F_6$ manifold. In Tb^{3+}:YAlG, levels are at 74 ± 4 cm^{-1}, 122 ± 4 cm^{-1} above the ground level; in Tb^{3+}:YGaG a level has been found which is at 46 ± 3 cm^{-1} above the ground level. The positions of the absorption bands of Tb^{3+}:YAlG are given in Table V.

4. Fluorescence Spectrum of Tb^{3+}: YAlG

The fluorescence spectrum has been recorded photoelectrically in the region between 4840 and 6320 Å. A large number of lines have been observed. Additional detailed spectral information was obtained from photographic measurements at 4.2 and 1.8°K, which were made available to us by Dr. D. L. Wood of this laboratory. All data are shown in Table VI.

The fluorescence spectrum at 1.8°K indicates the presence of a level of the $^5D_4$ manifold at $\sim$20 516 cm^{-1} above the ground state. Transitions to this level have not been observed in the absorption spectrum in the visible at 4.2°K.

III. ENERGY LEVEL DIAGRAM OF Eu^{3+}: YAlG AND Tb^{3+}: YAlG

The energy level diagram of Eu^{3+}:YAlG and Tb^{3+}:YAlG has been inferred from both the absorption and fluorescence spectra. The positions of the energy levels of these ions are given in Table VII.

IV. ANALYSIS OF THE SPECTRUM OF Eu^{3+}: YAlG AND Tb^{3+}: YAlG

Our experimental results indicate that the $(2J+1=3)$-fold degeneracy of the $^7F_1$ manifolds of both ions is completely removed by the crystal field. It is obvious that the symmetry of the crystal field is low. Since we are interested in the position of the Stark components

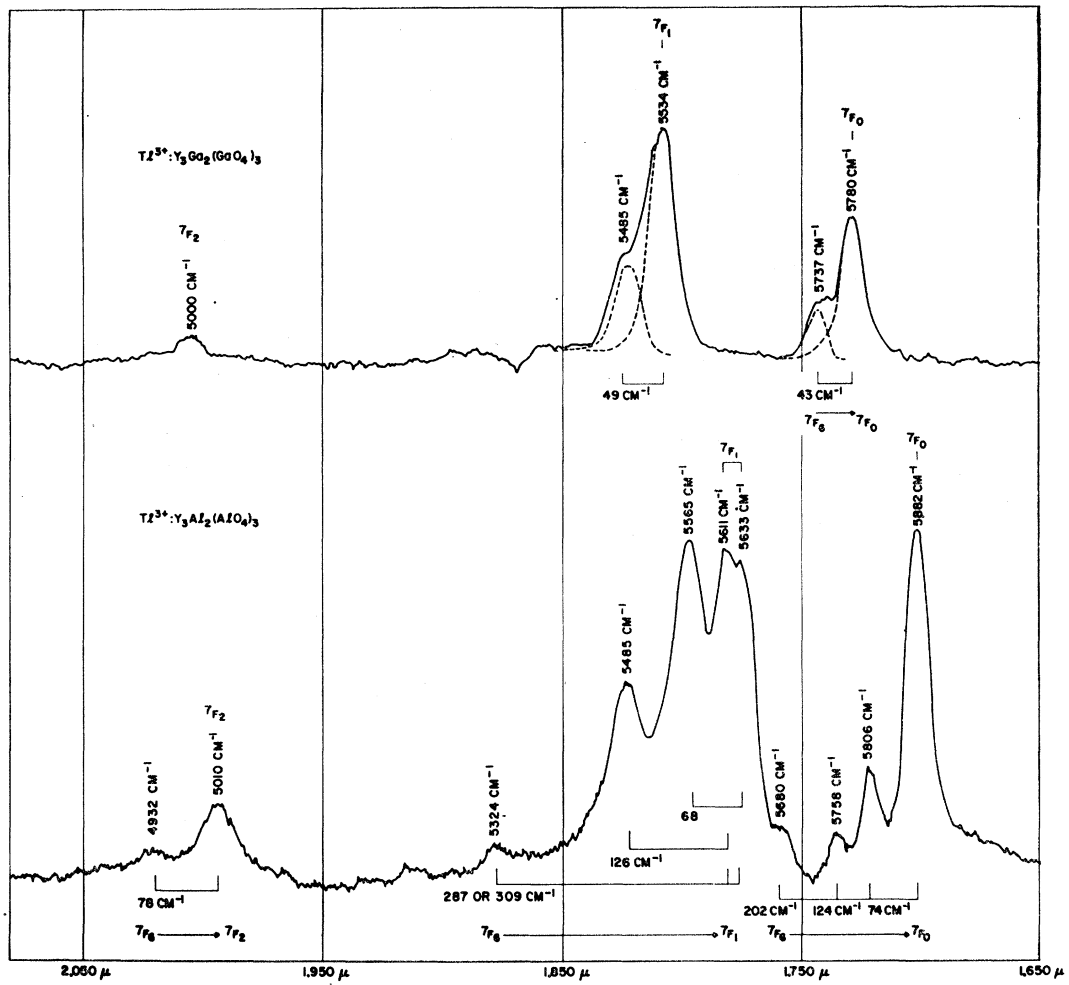

FIG. 6. The absorption spectrum of Tb^{3+}:YAlG and Tb^{3+}:YGaG between 2.05 and 1.65 μ at 30°K. Transitions originating in excited levels of the $^7F_6$ manifold and terminating on levels of $^7F_2$, $^7F_1$, and $^7F_0$ manifolds are indicated.

TABLE V. The absorption spectrum of Tb^{3+}:YAlG between 2130–5882 cm^{-1}. All transitions originate in the ground level.

Obs absorptions (cm^{-1})	Intensity[a]	Assignment
2130	st	$^7F_5$
2140	st	
2191	st	
2478	st	
2600	w	
2614	w	
3365	st	$^7F_4$
3380	st	
3413	st	
3488	st	
3605	st	
3697	m	
3725	st	
4397	m	$^7F_3$
4590	m	
4650	m	
4697	m	
4710	m	
5010	w	$^7F_2$
5611	m	$^7F_1$
5633	st	
5882	st	$^7F_0$

[a] w = weak; m = medium; st = strong.

of the J manifolds relative to their unsplit positions, it is only necessary to consider the contribution to the Hamiltonian which is produced by the crystalline electric field.

The crystal-field perturbation is usually[7] expanded in terms of the spherical harmonics:

$$V(r_k,\theta_k,\varphi_k)=\sum_n \sum_m \sum_k B_n{}^m r_k{}^n Y_n{}^m(\theta_k,\varphi_k), \qquad (1)$$

where

$B_n{}^m$ are constants,

$Y_n{}^m(\theta_k,\varphi_k)$ are spherical harmonics,

$n=6$ for $4f$ electrons.

The constants $B_n{}^m$ depend on the positions of the neighbors around the rare earth ion. Although these positions are not known for the rare-earth ions in the host-lattice YAlG, such data are available for the iron garnet.[7,11] The yttrium ions which are replaced by the rare-earth ions, occupy orthorhombic sites of the cubic

[11] G. Z. Menzer, Kristallografiya **69**, 300 (1929).

Table VI. Fluorescence of Tb^{3+}:YAlG. Fluroescence originates in levels of the $^5D_4$ manifold.

Obs (cm^{-1})	Series I 20 657-$\bar{\nu}$	20 646-$\bar{\nu}$	Obs (cm^{-1})	Series II 20 601-$\bar{\nu}$	20 589-$\bar{\nu}$	Obs (cm^{-1})	Series III 20 549-$\bar{\nu}$	Obs (cm^{-1})	Series IV 20 513-$\bar{\nu}$	Average	Assignment
						20 487	62	20 453	60	61	$^7F_6$
			20 530	71				20 443	70	70	
								20 304	207	207	
20 371		275	20 328		271			20 247	266	270	
20 215		431						20 080	433	432	
			20 145		444	20 100	449	20 072	441	443	
						18 420	2129	18 389	2124	2127	$^7F_5$
						18 410	2139	18 378	2135	2137	
18 483		2163	18 440	2161				18 354	2159	2161	
								18 325	2188	2188	
			18 255		2334			18 178	2335	2335[a]	
18 305	2352		18 235		2354			18 167	2346	2350[a]	
								18 048	2387	2387[a]	
			17 985		2064	17 947	2602	17 917	2596	2601	
						17 935	2614	17 906	2607	2611	
17 287		3359						17 148	3365	3362	$^7F_4$
17 258		3388	17 203		3387	17 167	3382	17 124	3389	3386	
								17 092	3421	3421	
								17 022	3491	3491	
			16 988		3601	16 942	3607	16 911	3602	3602	
			16 884	3717		16 831	3718	16 801	3712	3716	
16 239		4407				16 163	4386			4392	$^7F_3$
16 119	4538					16 017	4532			4535[a]	
						15 972	4577			4577	
			15 913	4688		15 867	4682			4682	
15 939		4707				15 842	4707			4707	
								15 067	5446	5446[a]	$^7F_1$
15 045	5612		14 987	5614				14 900	5613	5613	
15 026	5613		14 966	5634		14 922	5627			5631	
14 770	5880		14 728	5873		14 668	5881			5878	$^7F_0$

[a] Levels of ^7F manifolds not observed in the absorption spectrum in infrared

space group $O_h(10)Ia3d$. Eight oxygen ions located on the corners of a distorted cube are the closest neighbors. The B_n^m's in the iron garnet have been calculated by Dillon and Walker.[8] Their calculation shows that B_2^0, B_2^2, B_4^0, B_4^4, B_6^0, and B_6^4 are the most important terms. Recent crystal-field calculations on the splitting of J manifolds of Nd^{3+}:YAlG indicate[6] that the symmetry of the crystal field is approximately tetragonal. By employing the operator equivalent method of Stevens, Elliott, and Judd,[12–14] we can write the crystal-field Hamiltonian H_c as

$$H_c=\alpha[A_2^0Y_2^0+A_2^2(Y_2^{+2}+Y_2^{-2})]+\beta[A_4^0Y_4^0+A_4^4(Y_4^{+4}+Y_4^{-4})]+\gamma[A_6^0Y_6^0+A_6^4(Y_6^4+Y_6^{-4})], \quad (1a)$$

where α, β, γ are operator equivalent constants and

$$A_n^m=\langle r^n\rangle B_n^m \quad \text{with} \quad (r^n)=R(r)^2r^{n+2}dr.$$

It has been shown that some of the J states of the trivalent rare-earth ions depart quite drastically from Russell-Saunders coupling. These deviations are, however, small for the ^7F states of the Eu^{3+} and Tb^{3+}.[15]

The splitting of the $^7F_1$ manifold is directly related to the parameters A_2^0 and A_2^2. The position of the Stark components of this manifold as a function of the ratio A_2^2/A_2^0 is shown in Figure 7. Values of these parameters for Eu^{3+}:YAlG calculated for the three possible assignments, which are indicated with a, b, and c in Fig. 7, are given in Table VIII. From absorption and fluorescence spectra we have been able to establish the levels of the $^7F_1$ manifold of Eu^{3+}:$Y_3Ga_2(GaO_4)_3$[16] at 307, 345, and 388 cm^{-1} above the ground level. The parameters A_2^0 and A_2^2 calculated from these data, using the assignments corresponding to those for Eu^{3+}:YAlG, are also given in Table VIII.

It is straightforward to show that the crystal yield parameters A_2^0, A_4^0, A_4^4, A_6^0, and A_6^4 do not completely remove the $(2J+1)$-fold degeneracy of manifolds with integral values of J. Independent of the values of these crystal-field parameters one expects one doubly degenerate level for $J=1$ and $J=2$; two doubly degenerate levels for $J=3$ and $J=4$; and three doubly degenerate Stark components of $J=5$ and $J=6$ manifolds. Either the parameters A_2^2, A_4^2, and A_6^2 or J mixing can remove this degeneracy. Our experimental results indicate that some of the Stark components of Eu^{3+} and Tb^{3+}:YAlG and also of Eu^{3+}:YGaG are close together (Table VII). The number of these doublets agree with the number of doubly degenerate Stark levels of the ^7F manifolds in a field of tetragonal symmetry. The

[12] K. W. H. Stevens, Proc. Phys. Soc. (London) **A65**, 209 (1952).
[13] R. J. Elliott and K. W. H. Stevens, Proc. Roy. Soc. (London) **A218**, 553 (1953).
[14] B. R. Judd, Proc. Roy. Soc. (London) **A227**, 552 (1955).
[15] G. S. Ofelt, J. Chem. Phys. **38**, 2171 (1963).

[16] A complete analysis of the spectrum of Eu^{3+}:YGaG is discussed in the following paper [J. A. Koningstein and J. E. Geusic, Phys. Rev. **135**, A726 (1964)].

TABLE VII. Energy levels of Eu^{3+} and Tb^{3+}:YAlG.

Levels of Eu^{3+}:YAlG (cm^{-1})	Assignment	Number of Stark levels	Levels of Tb^{3+}:YAlG (cm^{-1})	Assignment	Number of Stark levels
0	$^7F_0$	1	0, 5	$^7F_6$	9
286, 307	$^7F_1$	3	61, 70		
455			116		
			207		
819	$^7F_2$	4	270		
902			432, 443		
1010, 1022					
1358					
			2128, 2138	$^7F_5$	9
1832, 1842	$^7F_3$	7	2161		
1915			2189		
1959			2335		
2000, 2008			2350		
2221			2387		
			2601, 2612		
2856, 2865	$^7F_4$	6	3364	$^7F_4$	7
2957			3383, 3417		
3137, 3147			3489		
3248			3603		
			3697, 3721		
3787, 3791	$^7F_5$	5			
3946			4394	$^7F_3$	6
4097[a]			4535		
4226[a]			4577		
			4590		
4976, 4983	$^7F_6$	8	4682, 4707		
5028					
5062			5010	$^7F_2$	1
5151					
5319			5446	$^7F_1$	3
5358			5612, 5632		
5445					
			5882	$^7F_0$	1
17 220	$^5D_0$	1	20 513	$^5D_4$	6
			20 548		
18 952	$^5D_1$	2	20 588, 20 601		
18 991					
21 356	$^5D_2$	3	20 546, 20 659		
21 448					
21 473					
24 639	$^5D_3$	4			
24 678					
24 683					
24 697					

[a] Split in Eu^{3+};$YGa_2(GaO_4)_3$.

observed splitting of the doublets indicates a small deviation from tetragonal symmetry. This deviation in the gallium garnet is larger than in the aluminum garnet, which implies that the parameters A_2^2, A_4^2, and A_6^2 are larger in the gallium garnet than in the aluminum garnet. As a result, we conclude that assignment *a* in Fig. 7 is the correct one for Eu^{3+}:YAlG.

The doublet-doublet spacing of the Stark components

TABLE VIII. Values of A_2^0 and A_2^2 for Eu^{3+}:YAlG and Eu^{3+}:YGaG.

Assignment[a] (cm^{-1})	Eu^{3+}:YAlG	Eu^{3+}:YGaG
(a) A_2^0	265	103.5
A_2^2	±52.5	±95
(b) A_2^0	−282	−135
A_2^2	±370	±107.3
(c) A_2^0	−248	−71.1
A_2^2	±422	±203

[a] For Eu^{3+}:YAlG, see Fig. 7.

of the $^7F_3$, $^7F_4$, and $^7F_5$ manifolds of Eu^{3+} and Tb^{3+}:YAlG have been employed to evaluate values of the crystal field parameters A_4^0, A_4^4, A_6^0, and A_6^4, neglecting the terms A_4^2 and A_6^2 for these ions. A comparison of observed and calculated splitting of the ^7F manifolds of both ions can be seen in Figs. 8 and 9. Values of the parameters which were used to calculate the splittings are given in Table IX.

Discrepancies between calculated and observed splittings are most pronounced for those Stark components

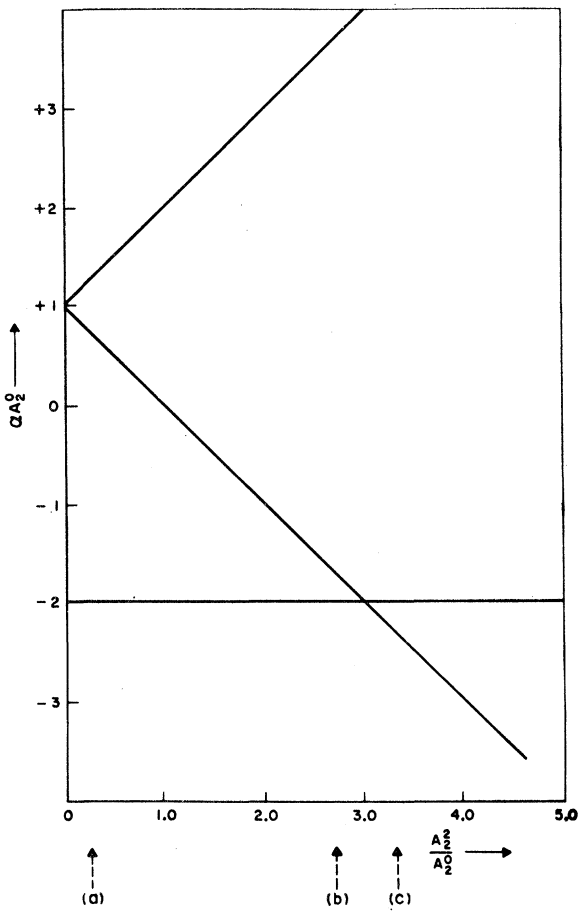

FIG. 7. The splitting of a $J=1$ manifold as a function of the ratio A_2^2/A_2^0. *a*, *b* and *c* refer to the assignments possible for the $^7F_1$ manifold levels of Eu^{3+}:YAlG.

TABLE IX. The values of the crystal-field parameters $A_n^m = \langle r^n \rangle B_n^m$ for Eu^{3+} and Tb^{3+} in YAlG in cm^{-1}.

	A_2^0	A_2^2	A_4^0	A_4^4	A_6^0	A_6^4
Eu^{3+}:YAlG	268	51	−190	950	94	−1150
Tb^{3+}:YAlG	266	50	−184	920	93	−1115

which are far removed from the center of gravity of the J manifolds. These discrepancies are probably due to J mixing. The disagreement between calculated and observed splitting is greatest for the $^7F_6$ state; such a disagreement was found by Judd for Eu^{3+} ethylsulfate.[17]

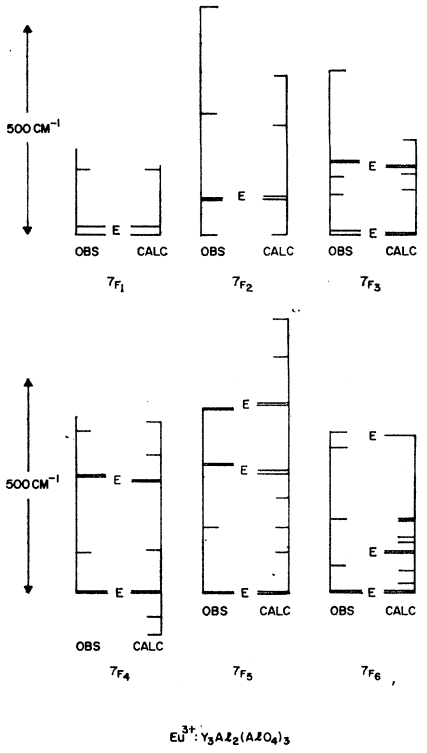

FIG. 8. Calculated and observed splitting of ^7F manifolds of Eu^{3+}:YAlG. E stands for the doublets and indicate in general the deviation of tetragonal symmetry.

[17] B. R. Judd, Mol. Phys. **2**, 4, 407 (1960).

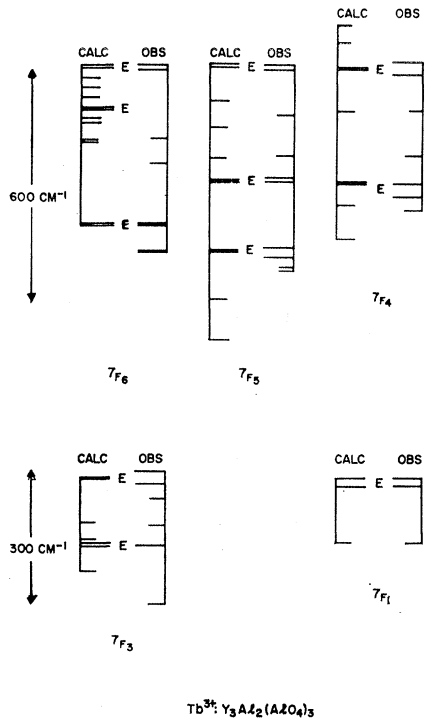

FIG. 9. Observed and calculated splittings of the ^7F manifolds of Tb^{3+}:YAlG. E stands for the doublets.

It should also be noted that the observed doublet spacing is larger than the calculated spacing. This is probably due to the fact that the parameters A_4^2 and A_6^2 are ignored in the calculations.

ACKNOWLEDGMENTS

The author wishes to thank Dr. J. E. Geusic for suggesting the problem and Dr. L. G. Van Uitert for supplying the crystals used in these investigations. He is indebted to Dr. D. L. Wood who made his fluorescence measurements available and to Dr. F. Varsanyi for valuable discussions. The technical assistance of I. Camlibel is acknowledged, while thanks are also due to Mrs. L. A. Needham who made computer programs which were used in the calculations.